2024 10th IEEE RAS/EMBS International Conference for
Biomedical Robotics and Biomechatronics (BioRob)
1-4 September 2024. Heidelberg, Germany

X-Ray-Guided Robotic Platform for Remote Control of Untethered Magnetic Robots Targeting Blood Clots in the Iliac Artery

Leendert-Jan W. Ligtenberg[1], Luuc de Jongh[1], H. Remco Liefers[2]
Dorothee Wasserberg[3,4], Emily A.M. Klein Rot[3], Doron Ben Ami[5], Udi Sadeh[5], Roger Lomme[6]
Gabriëlle G. M. Tuijthof[1,2], Oded Shoseyov[5,7], Pascal Jonkheijm[3,4], Michiel Warlé[6], and Islam S. M. Khalil[1,2]

***Abstract*— To date, the deployment of untethered magnetic robots (UMRs), activated by rotating permanent magnets, has been limited to controlled settings that do not replicate the dynamic conditions encountered *in vivo*. This study addresses this gap by exploring the challenges associated with transitioning UMRs from artificial environments to more realistic *ex vivo* scenarios, aiming to enhance their adaptability and functionality in dynamic physiological conditions. Initially, we develop an *ex vivo* endovascular thrombosis model in the iliac artery, facilitating the evaluation of clot removal through mechanical or chemical means. Subsequently, we deploy millimeter-sized bio-compatible UMRs and maneuver them toward blood clots using an X-ray-guided robotic platform. This demonstration showcases the operator's adept control in directing the UMRs precisely toward the blood clot, effectively engaging with it to reinstate blood flow. Utilizing cone-beam computed tomography scans for volume reconstruction of the clot (initial volume of $21.8\ \mathrm{mm}^3$) at specific time points, we illustrate that a significant volume reduction of 16% can be accomplished in under 30 minutes, all without the use of thrombolytic agents.**

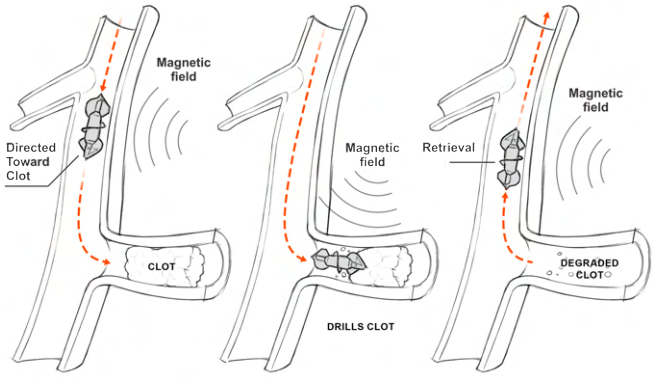

Fig. 1. An untethered magnetic robot (UMR) is deployed within an *ex vivo* endovascular thrombosis model situated in the iliac artery, employing precise control through magnetic fields. The UMR is navigated toward the clot, facilitating engagement and subsequent reduction in size, before being directed back toward the insertion point for retrieval.

I. INTRODUCTION

In the healthcare landscape, where the emphasis on minimally-invasive surgery is pivotal, addressing the challenges posed by acute ischemic stroke and occlusions in deep-seated vessels is paramount due to their significant impact on global morbidity and mortality. The pressing need for inventive solutions has driven the exploration of integrating robotics and electromagnetics, as demonstrated by the promising potential of wireless manipulation systems in medical interventions [1]. These wireless manipulation systems enable the control of untethered devices at the millimeter or micrometer scale without a tether, making occlusions in deep-seated vessels accessible (Fig. 1). While these untethered magnetic robots (UMRs) activated by rotating permanent magnets have demonstrated effectiveness in controlled settings [2], their application in the dynamic conditions of *in vivo* scenarios remains challenging, requiring advancements to enhance their adaptability and functionality.

This study builds upon significant advancements in the field of medical microrobotics, drawing inspiration from pioneering work presented by Kummer *et al.* [3]. In their research, an untethered magnetic device has been teleoperated in the retina using controlled magnetic fields. Notably, in such settings, the magnetic device can be controlled without the need for a medical imaging system due to accessibility to the retina. The exploration took a substantial leap forward when Gang *et al.* have successfully navigated RF-ablation catheters within pigs, showcasing the potential of magnetic guidance *in vivo* for treating cardiac arrhythmias [4]. This development set the stage for further innovation, exemplified by Carpi *et al.*'s magnetic steering of an endoscopic capsule inside living organisms, enhancing traditional capsule-based endoscopy [5]. Later, Keller *et al.* have successfully guided a magnetic endoscopy capsule in humans using modified magnetic resonance imaging system, highlighting the heightened effectiveness of endoscopic capsules through magnetic steering and field-gradient pulling [6].

[1]Department of Biomechanical Engineering, University of Twente, 7500 AE Enschede, The Netherlands.
[2]Technical Medical Centre, University of Twente, 7500 AE Enschede, The Netherlands.
[3]LipoCoat B.V., 7521 AG Enschede, The Netherlands.
[4]Laboratory of Biointerface Chemistry, Technical Medical Centre, University of Twente, 7500 AE Enschede, The Netherlands.
[5]Triticum Medical, 4726389 Ramat HaSharon, Israel.
[6]Radboud University Medical Center, 6525 GA Nijmegen, The Netherlands.
[7]The Hebrew University of Jerusalem, 76100 Rehovot, Israel.

The collaboration project is co-funded by the PPP Allowance made available by Health∼Holland, Top Sector Life Sciences & Health, to the University of Twente to stimulate public-private partnerships and the Twente University RadBoudumc Opportunities (TURBO) program 2022.

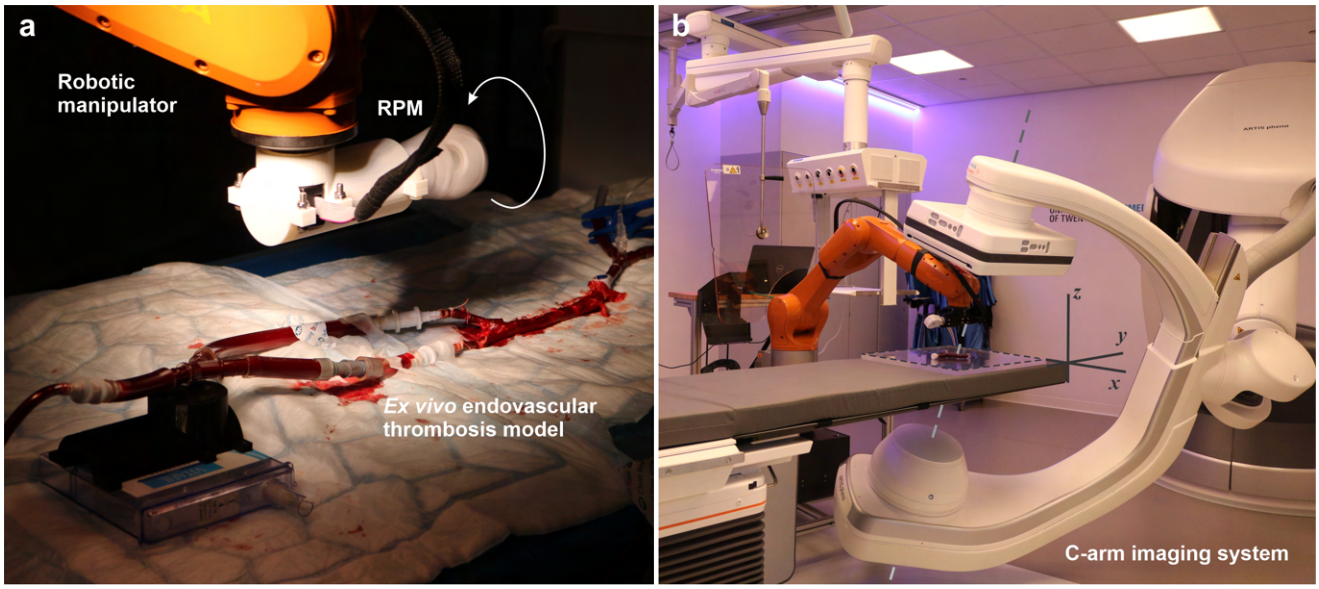

Fig. 2. Accurate blood clot targeting is demonstrated in an *ex vivo* endovascular thrombosis model within the iliac artery. (a) The iliac artery, connected to a circulation pump, exhibits a blood clot confined by a diameter-reducing wire. (b) The robotic platform integrates a C-arm imaging system and a wireless manipulation system, collaborating to achieve precise localization and wireless actuation. The UMR, situated within the iliac artery, is navigated using rotating magnetic fields.

Progress in magnetic guidance extends beyond the scope of endoscopy. Niedert *et al*. have presented an intriguing demonstration, utilizing a magnetically actuated tumbling strategy to guide a drug-loaded cylindrical robot in a rodent [7]. While the robot's tumbling motion allowed it to traverse the colon of the small animal, illustrating the potential for *in vivo* microrobots, it remained unclear how this capability could be effectively harnessed for engaging with actual diseased regions and implementing minimally invasive surgery. Expanding on this progress, Zhou *et al*. have demonstrated a bioprinting procedure using a magnetically controlled catheter [8]. This innovative technique facilitated the printing of 3-D silicone structures inside a mouse while undergoing magnetic steering. However, it is important to note that although these studies offer valuable insights, they may not offer comprehensive settings to test the interaction between the untethered robot and the diseased region or unwanted cells. To thoroughly assess the true potential of this technology, it is essential to engage with unwanted cells, at least in *ex vivo* settings.

This study aims to bridge this gap by investigating the challenges associated with transitioning UMRs (i.e., screw-shaped body with an affixed permanent magnet) from artificial environments to realistic *ex vivo* scenarios, with a particular focus on targeting blood clots within the iliac artery. Employing an X-ray-guided robotic platform for precise control [9], millimeter-sized UMRs are deployed to demonstrate their efficacy in engaging with blood clots and reinstating blood flow. Additionally, cone-beam computed tomography (CBCT) scans are employed for volume reconstruction of the clots at specific time points, revealing a volume reduction within 30 minutes—achieved without the use of thrombolytic agents. The outcomes presented herein not only contribute to the field of medical robotics but also hold promise for the development of minimally invasive procedures in the management of acute ischemic stroke and occlusions in deep-seated vessels. The rest of the paper is structured as follows: Section II offers insights into the *ex vivo* endovascular thrombosis model and the the robotic platform (Fig. 2). Our teleoperation control strategy and the hemobiocompatability of our UMRs are outlined in Section III. The *ex vivo* targeting of blood clots is presented in Section IV. Finally, Section V provides conclusions and outlines directions for future research.

II. OCCLUSIVE THROMBUS MODEL WITHIN AN X-RAY-GUIDED ROBOTIC PLATFORM

Engaging with a blood clot in an *ex vivo* setting requires overcoming several hurdles. First, the clot must be effectively trapped inside the blood vessel and continuously monitored to determine its size over time. Second, the UMR must be deployed and teleoperated toward the clot, achieving a satisfactory reduction in clot size. The wireless manipulation and medical imaging systems employed for actuation and clot reconstruction, respectively, must be scalable to the dimensions required for *in vivo* applications. These requirements are fulfilled through the utilization of an occlusive thrombus model and an X-ray-guided robotic platform.

A. Ex Vivo Endovascular Thrombosis Model

The aorta, renal arteries, and iliac arteries, along with blood, were obtained from euthanized sheep. The sheep (*Ovis aries*) were euthanized by injecting 15 mL of Euthasol (AST Pharma, Oudewater, the Netherlands) mixed with 5 mL of Heparin (5000 IU/mL, Leo Pharma, Ballerup, Denmark) into the jugular vein. After confirming death, the sheep was

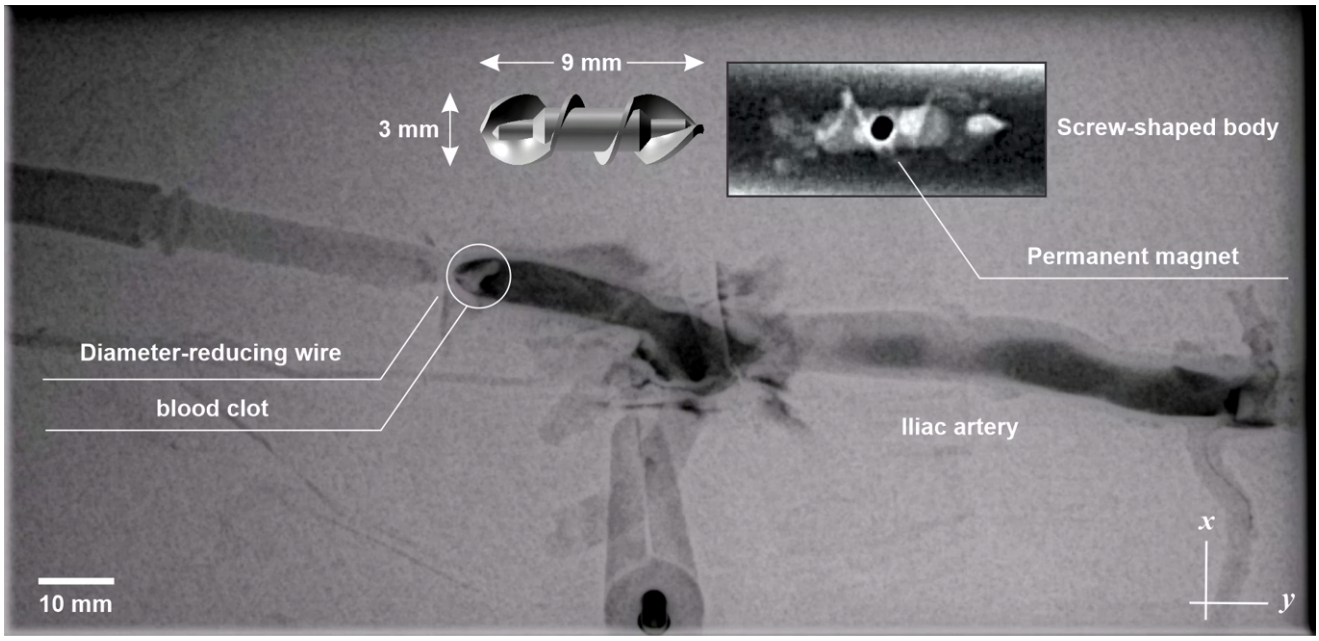

Fig. 3. The *ex vivo* endovascular thrombosis model is depicted through X-ray Fluoroscopy imaging while injecting a radiocontrast agent along the negative $\boldsymbol{y}$-axis. A diameter-reducing wire is used to trap the blood clot. The untethered magnetic robot (top-right inset) is inserted from the proximal end of the iliac artery and guided toward the blood clot.

positioned in a Trendelenburg position, and both the jugular vein and the carotid artery were ligated to allow blood to flow into a container. After collecting as much blood as possible, it was stored on ice. Subsequently, the sheep was transported to the laboratory, where the vessels were carefully excised and placed in a bag on ice for transport to the operating room, as depicted in Fig. 2(a). During transport, the blood and excised vessels were kept on ice.

In experimental settings, blood clots resembling a 1-day-old state are induced by promoting natural coagulation, allowing the blood to undergo thickening and form a semisolid mass. Subsequently, the clot is carefully inserted into the iliac artery and guided beyond the iliac bifurcation, as illustrated in Fig. 3. At this stage, a diameter-reducing wire is employed to precisely trap the clot within the vessel. While the interaction between the clot and arterial wall naturally results in a trapping response and resistance to sliding, the deliberate use of a diameter-reducing wire becomes necessary due to the smaller diameter of the blood clots compared to that of the vessel. This facilitates easier insertion and manipulation of the clots within the experimental setup. Upon establishing an occlusive thrombus model, the X-ray-guided platform is employed to systematically assess the interactions between the UMR and the clot.

B. X-Ray-Guided Robotic Platform

The X-Ray-Guided robotic platform, depicted in Fig. 2(b), incorporates an X-ray source and detector (Siemens Healthineers Artis Pheno, Erlangen, Germany) with three rotational degrees of freedom and one translational degree of freedom. While these degrees of freedom theoretically allow for the reconstruction of any environment, we intentionally constrain the configuration for real-time feedback essential for teleoperation at suitable frame rates. The X-ray source-detector axis (dashed gray line) maintains a fixed angle of 20° relative to the $\boldsymbol{z}$-axis (as per the frame of reference in Fig. 2(b)). This setup minimizes geometric blur while keeping the RPM out of the field of view, and a clinically acceptable signal-to-noise ratio is achieved using standard radiation levels, with a fluoroscopy dose rate of 0.35 mGy cm^2 s^{-1}, as shown in Fig. 3. Additionally, this oblique configuration expands the workspace, providing the robotic manipulator (KUKA KR-10 1100-2, KUKA, Augsburg, Germany) greater access over the iliac artery. Furthermore, the system is employed to reconstruct the volume of blood clots using CBCT scans.

III. X-RAY-GUIDED TELEOPERATION OF UNTETHERED MAGNETIC ROBOTS

To deploy the UMR inside the *ex vivo* model, three essential functionalities must be incorporated: biocompatibility, controlled response to an external stimulus (i.e., an external magnetic field), and the generation of a detectable signal with a sufficient contrast-to-noise ratio in the acquired X-ray Fluoroscopy images. Therefore, we fabricate screw-shaped bodies with an affixed permanent magnet (inset in Fig. 3) and coat their surface for biocompatibility.

A. Fabrication and Hemocompatibility

The UMRs were produced using Masked Stereolithography Apparatus (MSLA) with a 3D printer (Phrozen Sonic Mini 4K) and Phrozen Aqua-Gray 4K resin. The components were cleaned with isopropyl alcohol in an ultrasonic bath, post-cured using an Elegoo Mercury plus curing station, and coated with LipoCoat 4AC coating technology through manual dipcoating. Coated UMRs were left to dry overnight.

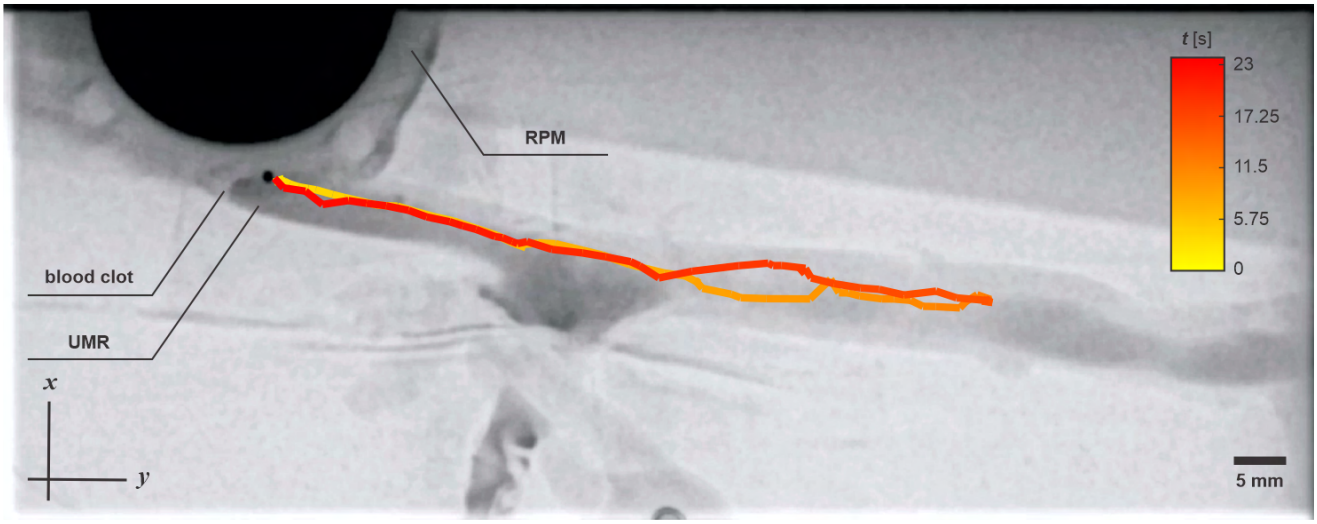

Fig. 4. The untethered magnetic robot (UMR) is deployed within an *ex vivo* endovascular thrombosis model located in the iliac artery. The UMR is guided to swim along the $\boldsymbol{y}$-axis away from the blood clot, and its motion is then reversed, directing it back toward the clot for engagement. The rotating permanent magnet (RPM) rotation axis is controlled robotically to move and guide the UMR. Please refer to supplementary multimedia.

The UMRs, with a minimum length of 9 mm and diameter of 3 mm, were constructed by assembling a 3D-printed screw-shaped body with an enclosed permanent magnet made of NdBFe Grade-N45 material (S-01-01-N Supermagnete, Gottmadingen, Germany). The cylindrical permanent magnet, measuring 1 mm in diameter and 1 mm in length, had a magnetic moment of 8.4×10^{-4} A m^2 and was positioned to enable the UMR to swim within blood upon rotation, following an external low-strength magnetic field of 5 mT. Biocompatibility studies, including protein fouling, and hemocompatibility assays, were conducted on the coated UMR material. Coated samples exhibited a significant reduction in protein adsorption and bacterial fouling compared to uncoated samples. Hemocompatibility tests were conducted by HAEMOSCAN BV, the coated samples passed all hemocompatibility tests, demonstrating high hemocompatibility and suggesting no issues with coagulation or complement activation during *in vivo* use.

B. Wireless Control and Targeting

The UMR is teleoperated to navigate toward the blood clot in the iliac artery, guided by X-ray Fluoroscopy images acquired at a real-time frame rate of 5 Hz. This operational frame rate facilitates precise control inputs from the operator, specifying the desired orientation for the RPM's rotation axis, the actuation frequency, and the direction of rotation of the RPM. The RPM's rotation axis (and its pose) is automatically controlled to facilitate the movement of the UMR within the iliac artery, a process dependent on the artery's geometry [10]. The actuation frequency has a linear relationship with the swimming speed of the UMR, provided it stays below the step-out frequency. Change of the direction of rotation of the RPM, allows for the UMR to swim back and forth along the vessel. This control input is particularly useful, as one direction of rotation enables the UMR to swim toward the clot, while the other direction reverses its motion after engagement.

Fig. 4 illustrates the targeting response of the UMR. In this experiment, the UMR is controlled to move along the $+\boldsymbol{y}$-axis against blood flow, and then its motion is reversed. Upon motion reversal, the UMR moves along the blood flow (in the -$\boldsymbol{y}$-axis) toward the clot, which prevents its advancement. When the UMR is controlled to move away from the blood clot, its swimming speed is measured to be 9.5 mm/s. In its path toward the blood clot, the swimming speed increases to 11.5 mm/s. The difference in forward and backward swimming velocity is attributed to the 20 mL/min blood flow, which is induced in the direction toward the blood clot.

In this trial, the UMR swims back and forth approximately 24 body lengths in approximately 20 seconds, at an actuation frequency of 9 Hz. At around 23 seconds, the UMR comes in contact with the blood clot, initiating its engagement with the fibrin network. At this point, several engagement strategies can be adopted to reinstate blood flow. One of these strategies is to drill through the blood clot using the propulsive thrust of the screw-shaped body. Alternatively, the UMR may be used to deploy a concentrated cargo of thrombolytic agent, breaking up and dissolving blood clots that impede blood flow. This paper investigates the first method.

IV. ENGAGEMENT WITH BLOOD CLOTS

To evaluate the impact of the UMR on the clot, we investigate two distinct groups. The first group involves measuring the blood clots without fragmentation using the UMR, while the second group involves mechanical fragmentation for 30 minutes. In each case, the volume of the blood clot is reconstructed using CBCT scans taken every fifteen minutes. Cross-sectional images were generated through CBCT reconstruction to determine the clot's volume over time, as shown in Fig. 5.

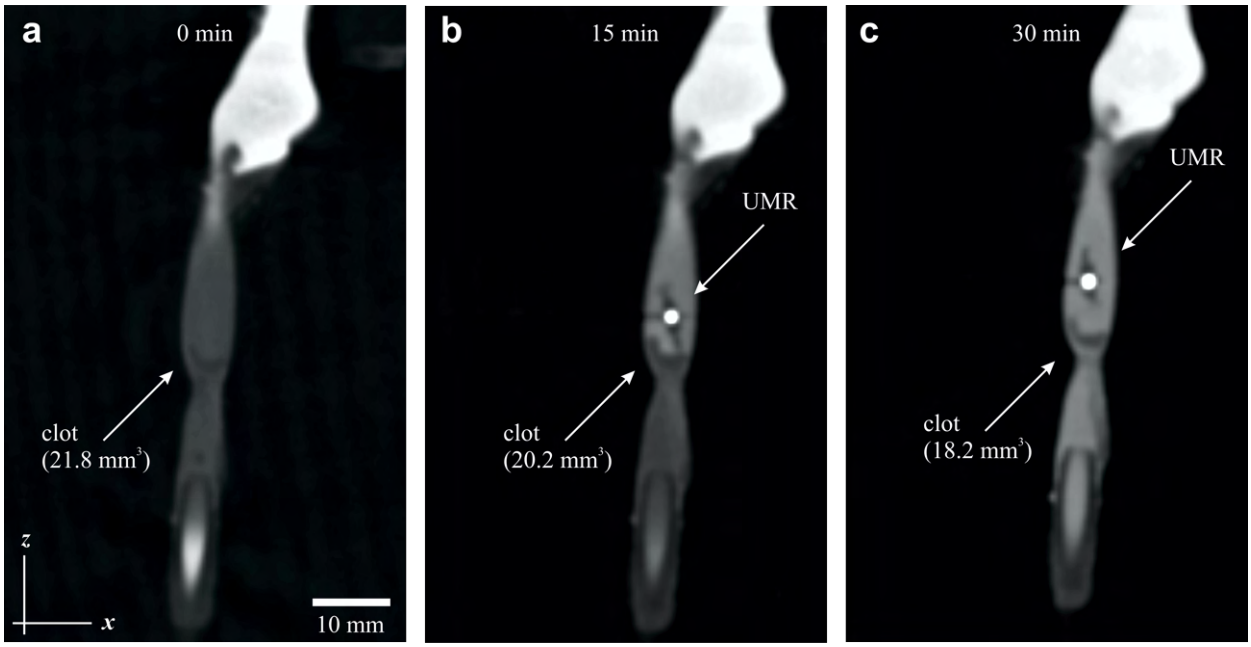

Fig. 5. Pre- and post-interventional CBCT scans are collected every 15 minutes to establish the control and the fragmentation measurement, respectively. The size of the blood clot is measured from reconstructed scans, with the bright region indicating the UMR. (a) Initial blood clot volume measured using volume acquisition CT is 21.8 mm^3. (b) After 15 minutes, the volume decreases to 20.2 mm^3. (c) Grinding the blood clot for 30 minutes results in a volume reduction of 16%, yielding a clot volume of 18.2 mm^3. Please refer to supplementary multimedia.

A. Pre-Interventional CBCT Imaging – Control

For the control, we measure the volume of the clot in the absence of any external stimuli, either mechanical or chemical. Blood clots are produced and trapped inside the iliac artery past the iliac bifurcation using the diameter-reducing wire. In the absence of clot-UMR interaction, the clot is reconstructed using CBCT scans every 15 minutes for 30 minutes. Our observations indicate minimal measurable change in the volume of the clot (Fig. 6). Therefore, the deployment of the UMR toward the clot and measuring the size of the clot versus fragmentation time can be assessed using this control measurement.

B. Post-Interventional CBCT Imaging – Fragmentation

The UMR is deployed and guided using controlled rotating magnetic fields toward the clot, as depicted in Fig. 5. In this trial, a new blood clot is inserted and trapped inside the iliac artery. The blood clot and the UMR are highlighted in the CBCT scan as the bright and dark regions, respectively. Upon reaching the blood clot site, the UMR is allowed to grind the clot for 30 minutes on the axial plane, Fig. 7, and CBCT scans are collected every 15 minutes to monitor the clot's size and assess the impact of the UMR. The propulsive thrust of the rotating screw-shaped UMR enables continuous engagement with the clot, as illustrated in Fig. 5. While the UMR is not permitted to advance forward and drill through the clot, the magnetic torque exerted on its magnetic dipole facilitates continuous rotational motion, resulting in a grinding action. Similarly to the swimming speed of the UMRs, the rate of clot removal is likely to depend on the rotational frequency of the UMR, particularly below its step-out frequency. In this trial, the UMR operates at 11 Hz with a 10 cm distance from the RPM actuator, resulting in a maximum magnetic field of 4 mT at the UMR's position.

Fig. 5(a) illustrates the initial interaction between the UMR and the blood clot, with a corresponding volume acquisition CT measurement of 21.8 mm^3. Following 15 minutes of uninterrupted grinding with the rotating UMR, the volume decreases to 20.2 mm^3, as depicted in Fig. 5(b), reflecting a 1.6 mm^3 reduction in clot volume. Finally, the volume of the blood clot decreases to 18.2 mm^3 after 30 minutes, as shown in Fig. 5(c). Therefore, this experiment indicates that the grinding action between the UMR and blood clot yields a volume reduction of 3.6 mm^3.

Volume acquisition CT measurement of the blood clot involves using CT imaging to capture a three-dimensional representation of the clot's volume, as shown in Fig. 6 and Fig. 7. In this context, the initial volume, measured at 21.8 mm^3, serves as a baseline. Subsequent CT scans at specific time intervals, such as 15 minutes and 30 minutes, provide insights into how the clot volume changes over time. The acquired images allow for a detailed assessment of the clot's structure and dimensions, enabling the evaluation of the impact of the UMR's grinding action on clot reduction.

At the initial time point ($t = 0$), the coronal plane displays a relatively blunt peak, and curved structure of the blood clot. However, after 30 minutes of continuous grinding, the peak near the top-left side of the clot has shrunk and become distinctively sharper, viewed from the coronal plane in Fig. 7. This observation indicates the localized impact of the UMR's grinding action on the clot's geometry, resulting in the formation of a more prominent features within the

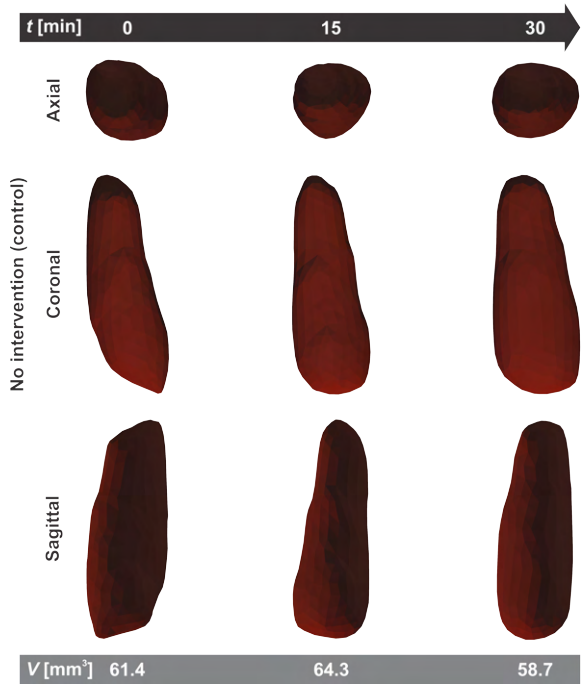

Fig. 6. Volume acquisition CT is employed to reconstruct the volume of the blood clot int the control measurement. The initial volume of the blood clot is 61.4 mm^3, and it decreases to 58.7 mm^3 after 30 minutes. The clot size exhibits minimal change within a relative measurement error of 5%.

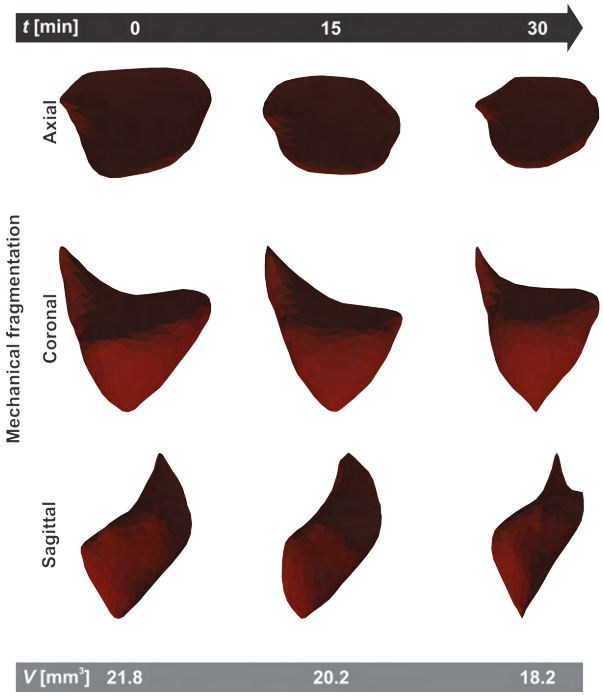

Fig. 7. Volume acquisition CT is employed to reconstruct the volume of the blood clot. The initial volume of the blood clot is 21.8 mm^3, decreasing to 18.2 mm^3 after 30 minutes of UMR fragmentation. The tapering of the blood clot suggests that the UMR exerts a pushing force on the clot during the fragmentation process, while oriented orthogonal to the axial plane.

clot structure. The axial and sagittal views further confirm that the UMR induces a tapered clot geometry that becomes progressively sharper with increased grinding time. This observation across multiple planes suggests a consistent and localized effect of the UMR's grinding action on the clot's overall shape.

V. CONCLUSIONS

Our study represents an important advancement in medical microrobotics through the introduction of thrombus degradation with biocompatible UMRs. The implementation of an *ex vivo* endovascular thrombosis model within the iliac artery, provides a vital tool for evaluating the efficacy of UMRs. These UMRs, featuring permanent magnets, exhibited precise real-time control in X-ray-guided interventions within the *ex vivo* iliac artery model. Integration of CBCT scans for precise volumetric reconstruction unveiled a remarkable 16% reduction in clot volume within just 30 minutes of UMR engagement. This pioneering approach holds immense potential for addressing acute ischemic stroke and vessel occlusions, opening avenues for advanced exploration in complex scenarios and future clinical applications. In future work, we aim to enhance the efficacy of the UMR's mechanical fragmentation approach by exploring a hybrid strategy that incorporates chemical lysis using thrombolytic agents. This involves investigating the potential benefits of either injecting or encapsulating thrombolytic agents with the UMR. The synergistic combination of mechanical and chemical approaches holds promise for optimizing clot dissolution, potentially improving the overall efficiency of the UMR in addressing vascular occlusions and acute ischemic stroke.

REFERENCES

[1] F. Carpi and C. Pappone, "Stereotaxis Niobe magnetic navigation system for endocardial catheter ablation and gastrointestinal capsule endoscopy," *Expert Rev. Med. Devices*, vol. 6, no. 5, pp. 487–498, 2009.
[2] T. W. R. Fountain, Prem V. Kailat, and J. J. Abbott, "Wireless control of magnetic helical microrobots using a rotating-permanent-magnet manipulator," in *Proc. IEEE Int. Conf. Robot. Autom.*, 2011, pp. 576–581.
[3] M. P. Kummer, J. J. Abbott, B. E. Kratochvil, R. Borer, A. Sengul, and B. J. Nelson, "OctoMag: An electromagnetic system for 5-DOF wireless micromanipulation," *IEEE Trans. Robot.*, vol. 26, no. 6, pp. 1006–1017, Dec. 2010.
[4] E. S. Gang et al., "Dynamically shaped magnetic fields: Initial animal validation of a new remote electrophysiology catheter guidance and control system," *Circ. Arrhythm. Electrophysiol.*, vol. 4, no. 5, pp. 770–777, Oct. 2011.
[5] F. Carpi, N. Kastelein, M. Talcott, and C. Pappone, "Magnetically controllable gastrointestinal steering of video capsules," *IEEE Trans. Biomed. Eng.*, vol. 58, no. 2, pp. 231–234, Feb. 2011.
[6] H. Keller et al., "Method for navigation and control of a magnetically guided capsule endoscope in the human stomach," *in Proc. 4th IEEE RAS EMBS Int. Conf. Biomed. Robot. Biomechatronics (BioRob)*, Jun. 2012, pp. 859–865.
[7] E. E. Niedert, C. Bi, G. Adam, E. Lambert, L. Solorio, C. J. Goergen, and D. J. Cappelleri, "A tumbling magnetic microrobot system for biomedical applications," *Micromachines*, vol. 11, no. 9, Sep. 2020.
[8] C. Zhou et al., "Ferromagnetic soft catheter robots for minimally invasive bioprinting," *Nature Commun.*, vol. 12, no. 1, 12 2021.
[9] L.-J. W. Ligtenberg, N. C. A. Rabou, et al., "Ex vivo validation of magnetically actuated intravascular untethered robots in a clinical setting," *Commun. Eng.*, vol. 3, no. 1, May 2024.
[10] L.-J. W. Ligtenberg, N. C. A. Rabou, et al., "Remote control of untetherd magnetic robots within a lumen using X-ray-guided robotic platform," in *Proc. IEEE Int. Conf. Robot. Autom.*, 2024, pp. 17763–17769.